Article:
Das, C, Read, DJ, Soulages, JM et al. (2014) Modeling of synthesis and flow properties of propylene-diene copolymers. Macromolecules, 47 (16). pp. 5860-5868. ISSN: 0024-9297

https://doi.org/10.1021/ma5011205

Modelling of synthesis and flow properties of propylene-diene copolymers

Chinmay Das,*,† Daniel J. Read,‡ Johannes M. Soulages,¶ and Pradeep P. Shirodkar§

School of Physics and Astronomy, University of Leeds, Leeds, LS2 9JT, UK, Department of Applied Mathematics, University of Leeds, Leeds, LS2 9JT, UK, Corporate Strategic Research, ExxonMobil Research and Engineering Company, Annandale, NJ 08801, and Global Chemical Research, ExxonMobil Chemical, Baytown, TX 77520

E-mail: c.das@leeds.ac.uk

Abstract

Copolymerisation with non-conjugated dienes offers an attractive route for introducing long-chain branching in polypropylene. From a simplified set of rate equations for such copolymerisation with a metallocene catalyst, we derive the probabilities of branch formation at different stages of the reaction in a semi-batch reactor. Using these probabilities, we generate an ensemble of molecules via a Monte Carlo sampling. The knowledge of the branching topology and segment lengths allows us to compute the flow properties of the resins from computational rheology. We compare our model predictions with existing experimental data, namely the molar mass distribution and small angle oscillatory shear response, for a set of resins with varying diene content.

*To whom correspondence should be addressed
†School of Physics and Astronomy, University of Leeds, Leeds, LS2 9JT, UK
‡Department of Applied Mathematics, University of Leeds, Leeds, LS2 9JT, UK
¶Corporate Strategic Research, ExxonMobil Research and Engineering Company, Annandale, NJ 08801
§Global Chemical Research, ExxonMobil Chemical, Baytown, TX 77520

The rheology data suggests that the entanglement time τ_e depends sensitively and in a well-defined fashion on the diene content.

1 Introduction

Small amounts of long-chain branching (LCB) in polymer resins drastically affect the melt flow properties and often lead to better processability[1,2]. Constrained-geometry catalysts[3], like metallocenes, offer high control on polyolefin synthesis. Metallocene catalysts can produce some LCB in polyethylene by creating macromonomers with reactive double bond through β-hydride elimination and subsequent reincorporation of macromonomers at a later time during the polymerisation process[4]. Polypropylene (PP) polymerisation using most metallocene catalysts, typically propagated through 1,2 insertion and terminated by β-hydrogen elimination, leads to a sterically congested vinylidene chain-end that prohibits further inclusion in another growing chain[5,6]. Copolymerisation with non-conjugated dienes[7–9] offers a viable route to introduce LCB in one-step PP synthesis and to enhance amount of LCB during polyethylene synthesis using catalysts that allow macromonomer insertion[10,11].

Copolymerisation with diene (mainly in the context of polyethylene synthesis) has been modelled previously using the method of moments[11–14], finite element models[15], and generating functions[16]. These models predict the different moments of the molar mass distribution and the average number of branches. Because the flow properties of branched polymer melts strongly depend on the topological connectivity of the segments, such models fail to predict how the synthesised resins would behave in flow.

Here, we consider a metallocene catalyst that by itself does not produce LCB during PP synthesis. With a simplified set of rate equations, we calculate the probabilities for branch formation from diene incorporation in a semi-batch reactor. We use a Monte Carlo sampling scheme to generate a representative set of *in silico* molecules with information

about the molar masses of the segments and the topological connectivities. This allows us to compute the response in flow from computational rheology[17–22] based on the tube model[23]. We use literature data[7] on isotactic-polypropylene synthesised using a metallocene catalyst in the presence of varying diene (1,9-decadiene) concentration in order to compare with the predictions of our modelling for the molar mass distribution and the flow properties (stress response in small oscillatory shear).

While, the model presented here is only valid for metallocene catalysts that do not produce LCB of their own, it is relatively straight-forward to extend our calculation to a more general case. We outline the changes required to include LCB from macromonomer inclusion in the discussion (Section 4).

2 Modelling of reaction kinetics

2.1 Reaction steps

We use a simplified reaction kinetics with only the steps dominant in determining the long-chain branching structure. They are adapted from the reaction kinetics considered for polyethylene synthesis with metallocene catalysts[4]. A schematic representation of the steps involved is shown in Fig. 1. The polymerisation starts when an activated catalyst binds to a monomer (Fig. 1a). Following,[24] we denote this end as the 'upstream' end of the segment (and the other end as the 'downstream'). The polymerisation proceeds with the addition of monomers at a constant rate (rate constant K_{p}). The unreacted diene is incorporated with a rate constant K_{pD}, creating a once-reacted pendant diene. A pendant diene can then be incorporated with a rate constant K_{DLCB} to create long chain branching. The catalyst detaches from the growing chain at a rate K_{T}. Though only a vinylidene termination is shown in Fig. 1, the chain end can have a different structure. The rate constant K_{T} encompasses all possible termination processes. Following[25], we consider that catalyst deactivation occurs during the termination step with a rate K_{d}.

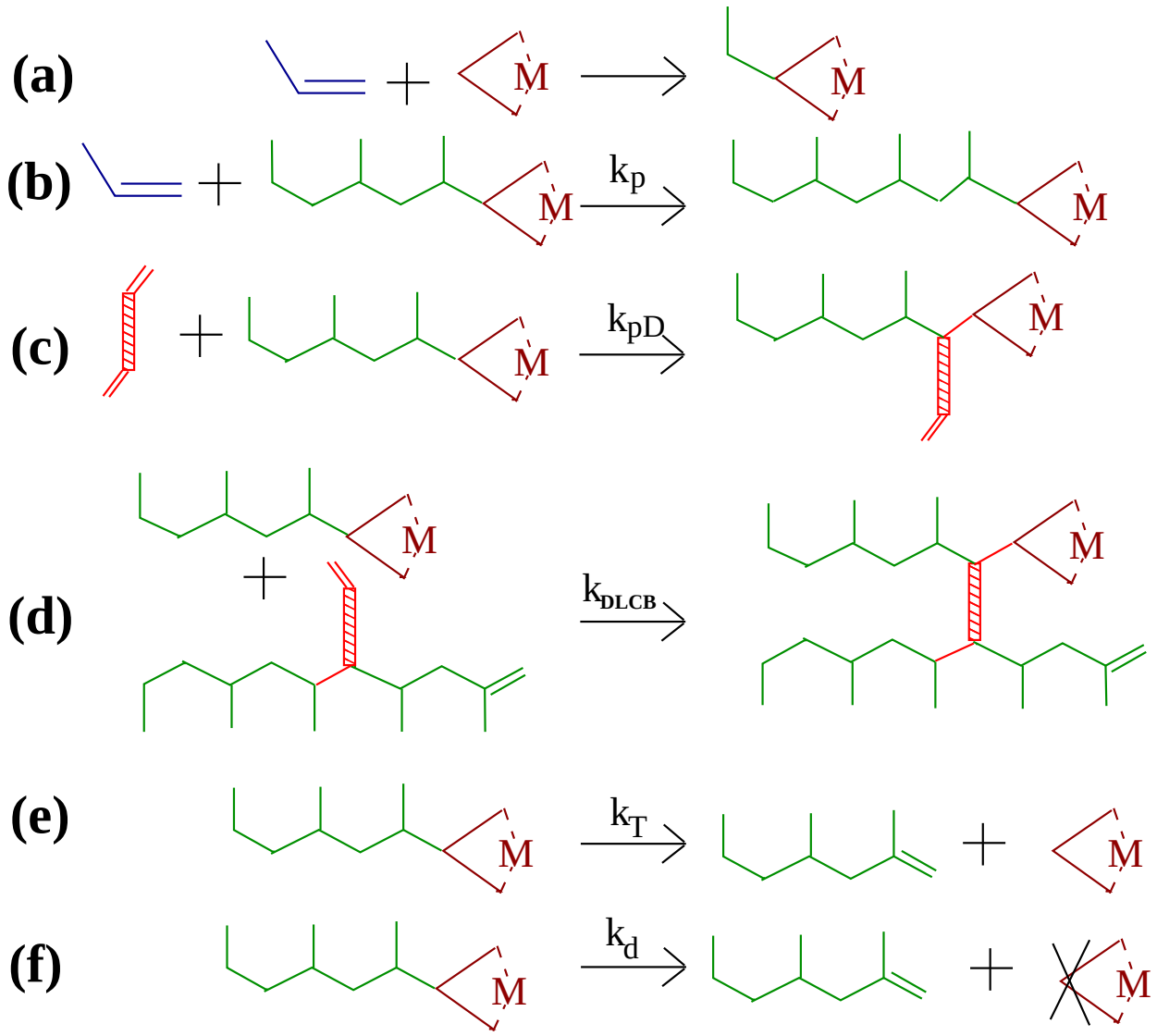

Figure 1: Schematic reaction steps considered for propylene-diene copolymerisation: (a) initiation, (b) monomer addition, (c) addition of diene to create once-reacted pendant diene, (d) long-chain branching by addition of a pendant diene, (e) termination, and (f) catalyst deactivation during termination.

2.2 Probabilistic sampling of the molecules

We consider a well-mixed semi-batch reactor, wherein an initial amount of non-conjugated diene and catalysts are added, and monomer concentration is kept constant until the end of the reaction. We wish to consider the final product at the end of the reaction and create an *in silico* ensemble of representative molecules. To achieve this goal, we select a single monomer from the reacted product and use the probabilities for the segment length and branching implied by the rate equations in order to construct the entire molecule containing the selected monomer. By repeating this procedure a number of times, we can generate an ensemble of molecules with the molar mass distribution and the branching topology consistent with the rate equations. Because we first pick a monomer on a polymer, the polymers are actually generated in a weight-biased fashion (i.e., the probability of selecting a molecule is proportional to the number of monomers contained in it). A similar approach has been used for generic free-radical polymerisation[26], dual catalyst metallocene polymerisation of polyethylene[25], and modelling of low-density polyethylene in a tubular reactor[21] or in a continuously stirred tank reactor[27].

In semi-batch conditions, the monomer concentration [M] is constant. But the concentration of (active) catalyst [Y](t) and that of unreacted diene [D](t) decay with time. It is convenient to introduce the monomer conversion x defined as

$$x \equiv \frac{[\mathrm{M_R}]}{[\mathrm{M}]}, \tag{1}$$

with [$\mathrm{M_R}$] being the concentration of reacted monomer, as a proxy for the time. Note that, since monomers are continuously replenished, the conversion x can be larger than unity. The time-evolution of the concentration of reacted monomer follows

$$\frac{d[\mathrm{M_R}]}{dt} = K_{\mathrm{p}}[\mathrm{M}][\mathrm{Y}](t), \tag{2}$$

relating time and conversion through

$$\frac{dx}{dt} = K_{\mathrm{p}}[\mathrm{Y}](t). \tag{3}$$

When expressed as a function of the conversion x, the rate equations are independent of the catalyst concentration and naturally account for the catalyst deactivation. The concentration of the reacted monomers grows at a constant rate in x. Thus, a randomly selected monomer would have reacted at a conversion x that is uniform between 0 and the final conversion x_f.

To calculate the length of the segment in which the selected monomer resides, we consider the ratio of the polymerisation to the termination rates to find the average number of monomers in the downstream direction of the selected monomer given by

$$\bar{N}_{\mathrm{d}n} = \frac{K_{\mathrm{p}}[\mathrm{M}]}{K_{\mathrm{T}}}, \tag{4}$$

and in the upstream direction by

$$\bar{N}_{\mathrm{u}p} = \frac{K_{\mathrm{p}}[\mathrm{M}]}{K_{\mathrm{T}} - K_{\mathrm{d}}}. \tag{5}$$

Because the polymerisation proceeds with the addition of monomers at a constant rate, the actual number of monomers in the segment is Flory distributed around these averages.

The concentration of the unreacted diene decays as

$$\begin{aligned} \frac{d[\mathrm{D}]}{dt} &= -K_{\mathrm{pD}}[\mathrm{D}][\mathrm{Y}], \\ \frac{d[\mathrm{D}]}{dx} &= -\frac{K_{\mathrm{pD}}}{K_{\mathrm{p}}}[\mathrm{D}], \\ [\mathrm{D}] &= D_0 \exp\left[-\frac{K_{\mathrm{pD}}}{K_{\mathrm{p}}}x\right]. \end{aligned} \tag{6}$$

Here, D_0 is the initial concentration of diene.

The concentration of once-reacted pendant diene [D_1] follows

$$\begin{aligned}
\frac{d[\mathrm{D_1}]}{dt} &= K_{\mathrm{pD}}[\mathrm{D}][\mathrm{Y}] - K_{\mathrm{DLCB}}[\mathrm{D_1}][\mathrm{Y}], \\
\frac{d[\mathrm{D_1}]}{dx} &= \frac{K_{\mathrm{pD}}}{K_{\mathrm{p}}} D_0 \exp\left[-\frac{K_{\mathrm{pD}}}{K_{\mathrm{p}}}x\right] - \frac{K_{\mathrm{DLCB}}}{K_{\mathrm{p}}}[\mathrm{D_1}], \qquad (7) \\
[\mathrm{D_1}] &= D_0 \frac{K_{\mathrm{pD}}}{K_{\mathrm{DLCB}} - K_{\mathrm{pD}}} \left(\exp\left[-\frac{K_{\mathrm{pD}}}{K_{\mathrm{p}}}x\right] - \exp\left[-\frac{K_{\mathrm{DLCB}}}{K_{\mathrm{p}}}x\right]\right). \qquad (8)
\end{aligned}$$

Considering a test chain growing at a conversion x, the density of pendant diene in the chain is given by the ratio of the addition rate of free diene to that of monomer as

$$\rho_{\mathrm{D1}} = \frac{K_{\mathrm{pD}}[\mathrm{D}]}{K_{\mathrm{p}}[\mathrm{M}]}. \qquad (9)$$

Only a fraction p_f of these pendant diene undergoes a second incorporation before the final conversion x_f is reached, which contributes to LCB. The probability of this second reaction is given by

$$p_f = 1 - \exp\left[-\frac{K_{\mathrm{DLCB}}}{K_{\mathrm{p}}}\left(x_f - x\right)\right]. \qquad (10)$$

The mean length to a pendant diene that subsequently reacted before x_f is given by

$$\bar{l}_{\mathrm{D1}} = \frac{1}{p_f \rho_{\mathrm{D1}}}. \qquad (11)$$

The conversion x_{D1} at which the pendant diene reacts for the second time is given by the cumulative distribution function (CDF)

$$\mathrm{CDF}(x_{\mathrm{D1}}) = \frac{1 - \exp\left[-\frac{K_{\mathrm{DLCB}}}{K_{\mathrm{p}}}\left(x_{\mathrm{D1}} - x\right)\right]}{p_f}. \qquad (12)$$

If we consider a chain growing at conversion x, we obtain the density of twice-reacted diene (i.e. density of long chain branches by incorporating a pendant diene that is already part of another segment) in the growing chain by comparing the pendant diene addition rate

to monomer addition rate as

$$\rho_{\mathrm{D2}} = \frac{K_{\mathrm{DLCB}}[\mathrm{D_1}]}{K_{\mathrm{p}}[\mathrm{M}]}. \tag{13}$$

The mean length to a branch-point created by incorporation of once-reacted diene ($\bar{l}_{\mathrm{D2}}$) is given by the inverse of this density ρ_{D2}.

To find out the conversion x_{D2} at which this incorporated pendant diene D_1 reacted for the first time, we note from Eq. 7 that the rate of creation of D_1 at conversion x_1 is $(K_{\mathrm{pD}}/K_{\mathrm{p}})D_0 \exp\left(-K_{\mathrm{pD}}x_1/K_{\mathrm{p}}\right)$ and the survival probability of D_1 created at x_1 at a later conversion x_2 is $\exp\left(-(K_{\mathrm{DLCB}}/K_{\mathrm{p}})(x_2 - x_1)\right)$. Considering a chain growing at conversion x, we end up with a cumulative distribution function of x_{D2} for a pendant diene incorporation given by

$$\mathrm{CDF}\left(x_{\mathrm{D2}}\right) = \frac{1 - \exp\left(-(K_{\mathrm{pD}} - K_{\mathrm{DLCB}})x_{\mathrm{D2}}/K_{\mathrm{p}}\right)}{1 - \exp\left(-(K_{\mathrm{pD}} - K_{\mathrm{DLCB}})x/K_{\mathrm{p}}\right)}. \tag{14}$$

2.3 Monte Carlo implementation

To generate a single molecule, we start by assigning the conversion for the selected monomer using a uniform random number x_c between 0 and the final conversion x_f. The number of monomers in the downstream and the upstream directions from the selected monomer are chosen from Flory distributions with averages respectively given by Eq. 4 and Eq. 5. The mean length to a branch-point created by incorporating a free diene that subsequently reacted a second time, $\bar{l}_{\mathrm{D1}}$, is calculated at the current conversion using Eq. 11. The mean length to a branch-point created by incorporating a pendant diene that was already part of a polymer segment, $\bar{l}_{\mathrm{D2}}$, is calculated from the inverse of the density in Eq. 13. The mean length to a branch-point $\bar{l}_B$ arising from either of these two possibilities is calculated using

$$\bar{l}_B = \left(\frac{1}{\bar{l}_{\mathrm{D1}}} + \frac{1}{\bar{l}_{\mathrm{D2}}}\right)^{-1}. \tag{15}$$

The distance to the next branch-point is calculated by generating a random number from the Flory distribution with the average given by $\bar{l}_B$. First considering the upstream direction,

if the distance to the branch-point is less than the end of the current segment, then we select a branch from incorporation of a free diene with probability $\bar{l}_{\mathrm{D1}}^{-1}/\left(\bar{l}_{\mathrm{D1}}^{-1}+\bar{l}_{\mathrm{D2}}^{-1}\right)$. Else, the selected branch is the result of the incorporation of a pendant diene. In the first case (incorporation of free diene), the incorporated diene would have reacted at a later conversion x_{D1} calculated by equating the CDF given by Eq. 12 to a uniform random number between zero and one and inverting the resulting algebraic expression. From this branch-point, we grow segments in both the downstream and upstream directions at this new conversion. Similarly, if the branching is due to incorporation of a pendant diene, the earlier conversion x_{D2} at which the diene first reacted is estimated from Eq. 14 and new segments are grown in either directions at the branch-point. We continue adding branch-points until the selected distance to the next branch-point is beyond the end of the current segment. The same procedure is repeated in the downstream direction. The algorithm is recursive in the sense that once we have considered a branch-point and added new segments, these new segments themselves were branched with their respective conversions. For PP-diene copolymerisation, the length of the diene is effectively zero compared to the chain lengths and the branch-points effectively act as tetra-functional junctions. To conform with the data structure of our computational rheology predictor[19], we keep a zero length segment at the branch-point. The whole procedure is repeated multiple times in order to generate an ensemble of molecules that follows the reaction kinetics considered here.

2.4 Broad monomer addition rate

Metallocene catalysts are considered to be single site. Considering polymerisation without diene, monomer addition at a fixed rate predicts a Flory distribution of linear segments with a polydispersity index (PDI, defined as the ratio of the weight average molar mass to the number average molar mass) of 2. However, often resins synthesised with metallocene catalysts show a PDI significantly larger than this ideal value of 2. In a well-mixed reactor, this broadening of molar mass has been modelled as the result of multiple catalysts with

different rate constants (each individually producing segments with PDI=2). In this work, we consider a variant of this by allowing the catalysts to have a continuous distribution of monomer addition rate constants K_{p} given by some probability distribution $\phi(K_{\mathrm{p}})$. The reason for such a distribution may involve small variations in steric or electronic conditions among the individual catalyst sites and is likely to result in a continuous distribution rather than discrete, well-separated values. We further assume that the diene addition rate constant, K_{pD}, is proportional to the propylene addition rate constant, K_{p}. Assuming that all other rate constants do not vary in between catalyst sites, the probabilities calculated in the case of single value of K_{p} survive with minimal modification in the Monte Carlo implementation. The catalysts with higher K_{p} values produce more polymers and hence the first selected segment is given a propagation rate constant from a biased distribution $\psi(K_{\mathrm{p}}) \equiv K_{\mathrm{p}}\phi(K_{\mathrm{p}})/\bar{K}_{\mathrm{p}}$, with $\bar{K}_{\mathrm{p}}$ being the average of K_{p} over the distribution $\phi(K_{\mathrm{p}})$. Considering branching from incorporation of a free diene that eventually is incorporated for the second time at a later conversion by another growing chain, the number of such chain follows the number of active catalysts. Hence, at a branch-point created from free diene incorporation, the newly incorporated segments get their K_{p} from the distribution $\phi(K_{\mathrm{p}})$. Our assumption that both the monomer addition and the diene addition rate constants vary in the same way among the catalyst sites leads to segments with higher K_{p} also incorporating more diene. Thus while considering branch-points due to the incorporation of a pendant diene, we assign K_{p} to the new segments from the biased distribution $\psi(K_{\mathrm{p}})$.

In our implementation, we choose a log-normal distribution for $\phi(K_{\mathrm{p}})$ centred around the average $\bar{K}_{\mathrm{p}}$, with a polydispersity index PDI(K_{p}) defined as the ratio of the second to the first moments. The choice of a log-normal distribution ensures the positivity of K_{p} and gives an analytical expression for $\psi(K_{\mathrm{p}})$, which, in this case, is yet another log-normal distribution.

3 Results

3.1 Molecular structure

To determine the effect of the initial diene concentration on the molecular structure, we used the algorithm outlined in the previous section in order to generate numerical ensembles of molecules. We chose the following parameters: [M] = 0.4 g/mol, $K_{\mathrm{p}} = 650\,\mathrm{L/mol\text{-}s}$, $K_{\mathrm{pD}} = 180\,\mathrm{L/mol\text{-}s}$, $K_{\mathrm{DLCB}} = 45\,\mathrm{L/mol\text{-}s}$, $K_{\mathrm{d}} = 10^{-4}\,/\mathrm{s}$, and $K_{\mathrm{T}} = 0.085\,/\mathrm{s}$. These rate constants are the same as those we use to describe some experimental resins in the next subsection. At this stage of the calculations, we consider a single monomer addition rate constant for all the catalysts, i.e. PDI(K_{p}) = 1. We fix the final conversion $x_f = 1$. For a range of initial diene concentrations D_0, in each case, we generate 5×10^5 molecules.

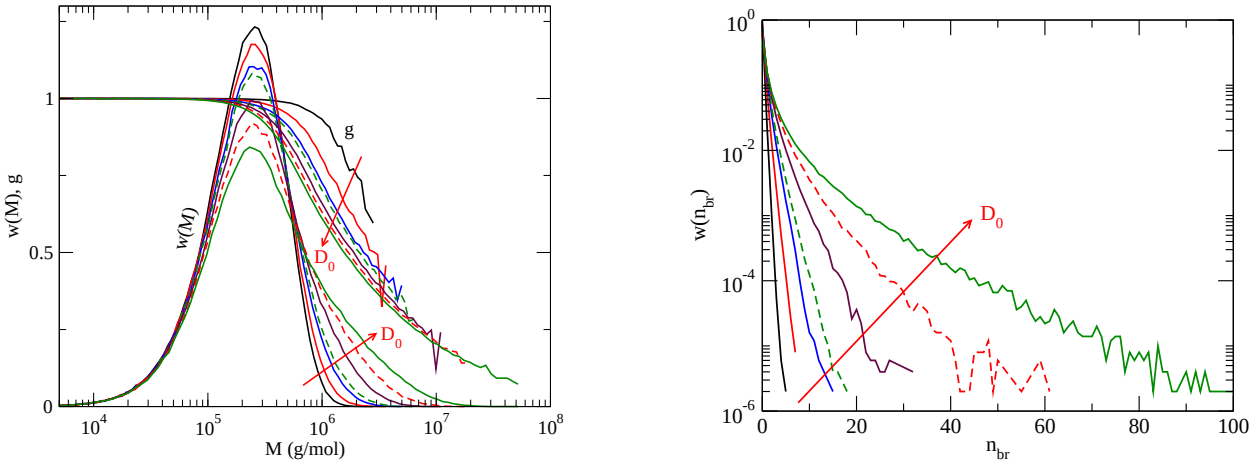

Figure 2: (a) Molar mass distribution w(M) and the radius of gyration contraction factor g for initial diene concentrations $D_0 = 10^{-4}$, 4×10^{-4}, 8×10^{-4}, 10^{-3}, 1.5×10^{-3}, 2×10^{-3}, and 2.5×10^{-3} mol/L. (b) Weight fraction of molecules having a certain number of branches $\mathrm{n_{br}}$. The initial diene concentrations are the same as in (a). In both plots, the arrows indicate increasing values of D_0.

The molar mass distributions calculated from the generated molecules are shown in Fig. 2a for several values of D_0. With increasing D_0, the molar mass distribution becomes broader and shows a more and more pronounced high-molar mass tail. Also shown in the figure are the radius of gyration contraction factors, g, defined as the ratio of the square of the radius gyration of the molecules to that of linear molecules having the same molar mass.

The g-values at high molar mass are significantly lower than 1, signifying highly branched structures. Fig. 2b shows the weight fractions of molecules having a particular number of branches for the same values of D_0.

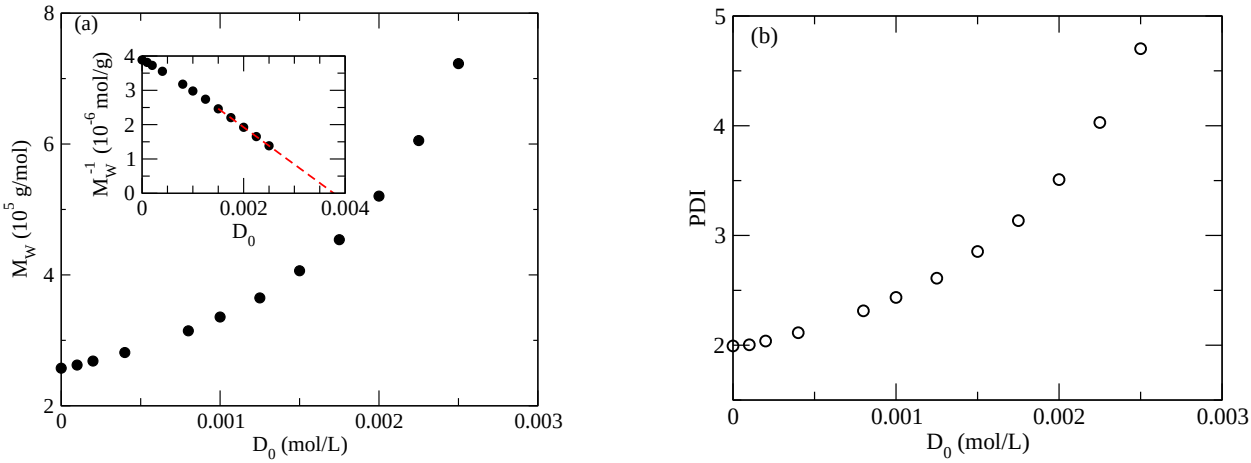

Figure 3: (a) Dependence of the weight average molar mass (M_W) on the initial diene concentration D_0. Inset: Plot of the inverse of the weight average molar mass as a function of D_0 and linear fit using the five highest diene concentration samples. (b) Polydispersity index of the resins as a function of D_0

Both the weight average molar mass (M_W) and the polydispersity index (PDI) increase with D_0 (Fig. 3a,b). The inset in Fig. 3a shows the inverse of M_W plotted as a function of D_0. By fitting a straight line through the calculated values of $1/M_W$ for the five highest diene concentrations, we can estimate a critical diene concentration $D_0^c \simeq 0.0038\,\mathrm{mol/L}$, for which our interpolation predicts a diverging molar mass or gel point.

Fig. 4 shows representative molecular structures for the molecules having a small number of branches. Neglecting the small length of the diene-bond, each of the branch-points can be assimilated to tetra-functional junctions. Thus, the molecule with a single branch-point is a 4-arm star. Molecules with two branch-points are q=3 pompom molecules[28]. Molecules with higher branch content are similar to comb polymers. Both ends of these molecules have 3 dangling arms and they contain a number of *side-arms*, occurring in pairs at the same point, on the *backbone*. Because of the random nature of diene-induced branching, the segments forming the molecules are typically polydisperse.

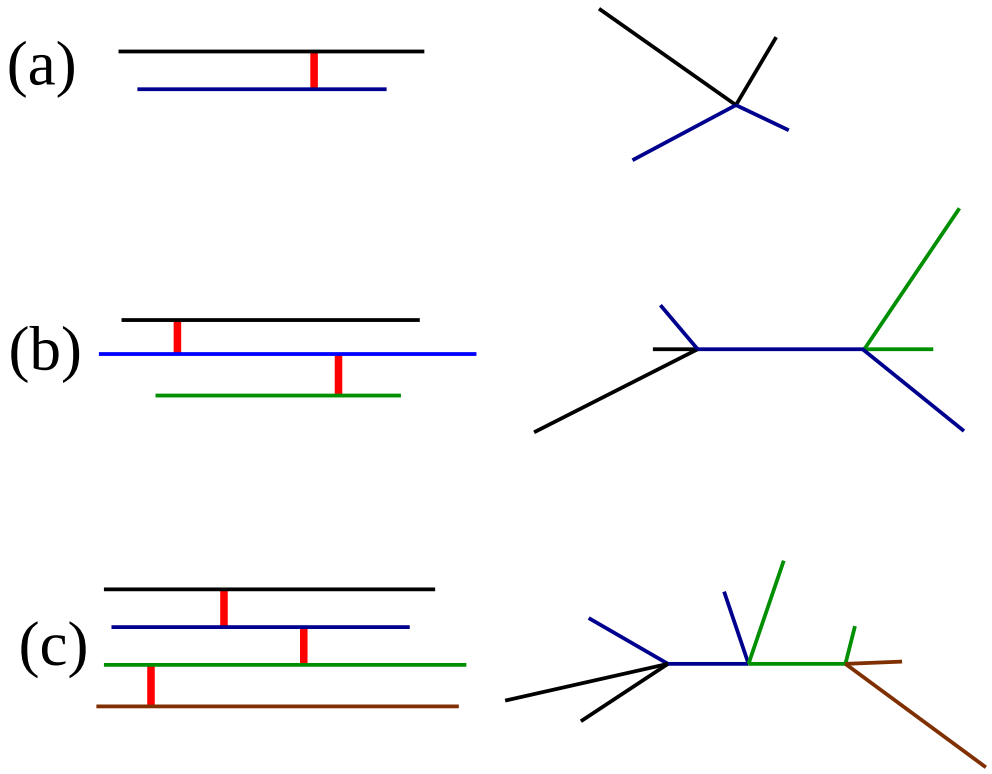

Figure 4: Topological shapes for propylene-diene copolymers. On the left, we show the segments generated at a given catalyst site as horizontal lines. Vertical short segments indicate reacted dienes forming bonds between the segments. On the right, we treat the dienes as tetra-functional branch-points and render the molecules differently. (a) A single diene bond creates a 4-arm star molecule. (b) With two diene bonds, the molecule is a pompom molecule with 3 dangling arms on both ends. (c) Molecules with more than two diene bonds are comb-like.

3.2 Comparison with experiments

We consider literature data[7] on four polypropylene samples synthesised with 1,9-decadiene using a metallocene catalyst and semi-batch conditions. This particular metallocene catalyst generates only linear polymers in the absence of diene. The diene concentrations used in the synthesis of the resins are summarised in Table 1. From the solubility of propylene in toluene[29], we estimate the monomer concentration to be [M] = 0.37 mol/L at the reaction temperature (40°C) and pressure (1 atm). For all samples, the initial catalyst concentration was the same (0.5 μmol in a volume of 150 mL) and the reaction was quenched after 30 minutes. From the reported amounts of polymer produced and the monomer concentrations, we can calculate the final conversion x_f for the samples and they are shown in Table 1. The values of x_f varies slightly across the samples suggesting slight variations in the monomer addition rate $\bar{K}_{\mathrm{p}}$ (an alternative explanation could be small variations in the fraction of active catalyst).

Table 1: Polymerisation reaction conditions and resin molar mass for propylene-decadiene copolymers considered in Ref.[7]. † Conversion x_f is calculated from the mass of the synthesised polymer assuming a monomer concentration 0.37 mol/L. Monomer is continuously replaced in a semi-batch reactor. Thus x_f, the ratio of reacted monomer to equilibrium unreacted monomer concentration in solution, can be larger than 1.

Resin	Diene conc. (mmol/L)	Conversion $x_f{}^{\dagger}$	M_w (kg/mol)	PDI
PP1	0	3.561	224.6	2.5
PP2	0.354	3.475	264.0	3.1
PP3	1.06	3.6036	879.2	8.0
PP4	1.77	3.475	1257.5	13.1

Our modelling suggests six different rate constants that affect the molecular structure: $\bar{K}_{\mathrm{p}}$, PDI(K_{p}), K_{pD}, K_{T}, K_{DLCB}, and K_{d}. In fact, all the expressions in section 2 use ratios of the rate constants involving $\bar{K}_{\mathrm{p}}$. It is possible that the five surviving parameters are not independent in determining the long-chain branching structure (i.e. different combinations of these five parameters may result in similar branching structure). For example, increasing K_{pD} and simultaneously decreasing K_{DLCB} can lead to a situation where the diene-induced

branching structure remains unchanged. In our fitting exercise, we found similar quality of fits with multiple sets of rate constants.

A set of rate constants that gives simultaneous good fit of the molar mass distributions of all the resins is $\bar{K}_{\mathrm{p}} = 650\,\mathrm{L/(mol\text{-}s)}$, $\mathrm{PDI}(K_{\mathrm{p}}) = 1.59$, $K_{\mathrm{pD}} = 180\,\mathrm{L/(mol\text{-}s)}$, $K_{\mathrm{DLCB}} = 45\,\mathrm{L}\ /\mathrm{(mol\text{-}s)}$, $K_{\mathrm{T}} = 0.085\,/\mathrm{s}$, and $K_{\mathrm{d}} = 10^{-4}\,/\mathrm{s}$ (Computational details are presented in an Appendix to this paper.) The predicted molar mass distributions for the resins along with the experimental data from[7] are compared in fig. 5. The inset in the figure uses logarithmic scale for both axes to highlight the large molar mass tail in the PP3 and PP4 resins. Comonomers are known to change catalyst rate constants[30] and improvements on the fits for the individual resins are possible by varying the rate constants independently for each of the resins.

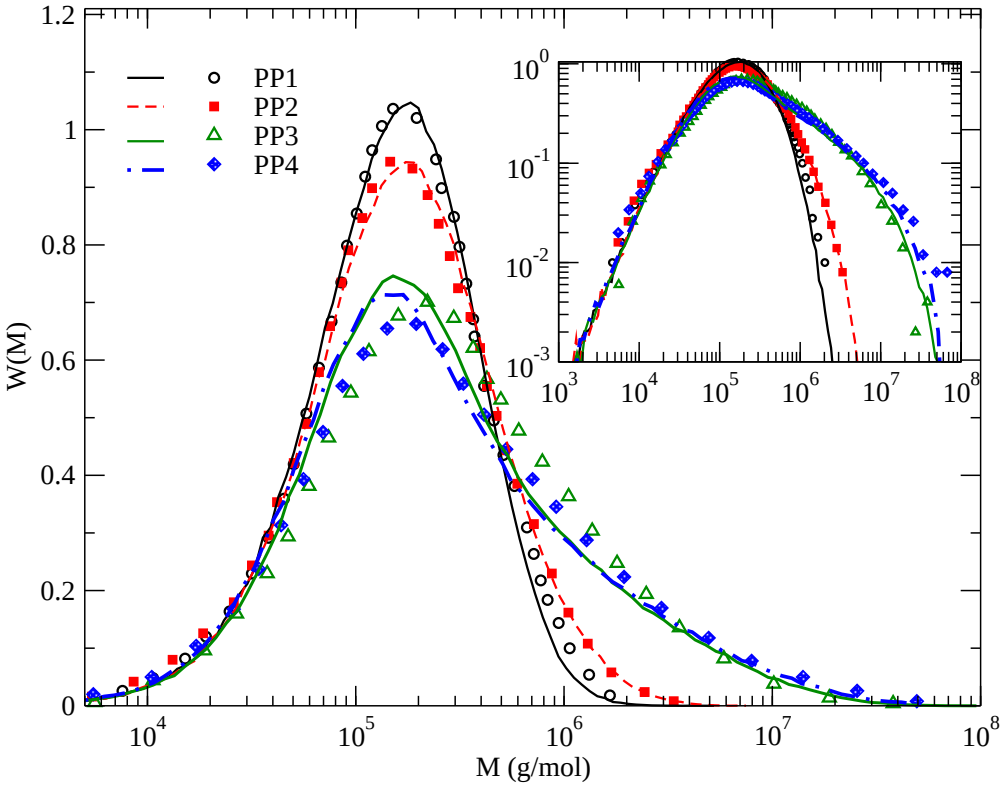

Figure 5: Molar mass distribution of the propylene-diene resins. Our modelling results are shown with lines. The inset shows the same plot with the y-axis in a log-scale to highlight the large molar mass tails in the samples. (Gel permeation chromatography data (symbols) are reproduced with permission from Ref.[7], Ye, Z.; AlObaidi, F.; Zhu, S. *Ind. Eng. Chem. Res.*, **2004**, 43, 2860-2870. Copyright (2004) American Chemical Society.)

Rheological measurements are extremely sensitive to small amounts of long chain branch-

ing and often predicting the rheological response is a more stringent test for the correct branching structure compared to predicting the molar mass distribution measured with gel permeation chromatography. We use the polymer molecular structures generated from our Monte Carlo program to compute the visco-elastic moduli using the BoB software[19,31] and compare our predictions with the experimental small angle oscillatory shear (SAOS) data from[7]. The BoB model has been used to successfully predict the linear viscoelasticity of a number of branched model and industrial resins, including well-defined model polymers that eventually lead to gelation[32,33] like the propylene-diene resins considered here.

Briefly, the tube theory[23] considers a given polymer molecule in a melt as being confined in a tube-like potential representing the topological uncrossability constraint due to all the other molecules. After a small step strain, considered as an affine deformation down to the length scale of the tube diameter, the stress is relaxed by the molecules moving out of their deformed tube constraints. For a branched molecule, the relaxation starts from the free chain ends via star-like arm retraction[34]. Completely retracted segments assign localised frictions, hindering the relaxation of the *backbone* segments at longer timescales. A segment with several such friction points from retracted side-arms (compound arms), itself retracts with the effective pivot point of retraction following a Rouse dynamics towards the centre of the molecule[19]. Eventually, when the unrelaxed part of the molecule becomes linear, the surviving stress is relaxed by reptation, a faster mechanism than arm retraction. Since the topological constraint of the tube potential is determined from the molecules which themselves are relaxing, the tube potential softens with the amount of relaxed material. This is modelled via phenomenological tube dilation, wherein the tube diameter depends on the amount of unrelaxed material through a power-law dependence[35,36]. The entanglement density experienced by the segments due to the dilated tube ('supertube') follows the fraction of unrelaxed material except at times when a significant fraction of material relaxes abruptly. If such a rapid relaxation of some material takes place, the entanglement density responds via a comparatively slow constraint release Rouse process[36,37]. Trying to predict the stress decay

in star-linear blends,[37] found that holding the tube diameter constant during the constraint release Rouse process gave a good description of the experimental data. When the resin considered contains only a small fraction of highly branched molecules, this prescription seems to break down. In this work, we consider that the tube diameter follows the entanglement density as defined by the "supertube" during the constraint release Rouse process. The dynamic tube dilation makes the relaxation of all the molecules in the melt coupled, frustrating analytical solution for molecules having polydispersity both in the segment length and the branching topology. Computational rheology[17–19] considers an ensemble of molecules and, after an imaginary small step strain, follows the relaxation of the molecules in discrete small (logarithmic) time steps updating the tube potential after each time step considering the contribution of all the molecules.

This relaxation theory requires two chemistry-independent and dimensionless parameters related to the dynamic tube dilation (α chosen to be 1) and the branch-point hop size (p chosen to be $1/\sqrt{40}$). These are the most commonly used values with the BoB algorithm[19,38]. Besides these two parameters, there are two other, chemistry dependent fitting parameters, namely the entanglement molar mass M_e and the entanglement time τ_e. The entanglement molar mass M_e is related to the plateau modulus (G_0) from rubber elasticity theory by $G_0 = (4/5)\rho RT/M_e$. Here, ρ is the density of the resin, R the universal gas constant, and T the absolute temperature. Using the measurement temperature of 190°C, the density $\rho = 0.766\,\mathrm{g/cc}$ and the reported plateau modulus $G_0 = 427000\,\mathrm{Pa}$[39], we estimate $M_e = 5520\,\mathrm{g/mol}$. We fit the SAOS data of PP1 to estimate the entanglement time $\tau_e = 1.15\times10^{-7}s$ (Fig. 6a). With the same choice of M_e and τ_e, we can describe the viscoelastic moduli of the iPP linear resin in[39].

The same values of M_e and τ_e fail to predict the SAOS data for the other resins. In Fig 6a, we show the frequency dependent viscoelastic moduli and our predictions with τ_e chosen independently for each of the samples. Fig 6b shows the frequency dependent complex viscosity for a blend of PP4 in the linear PP1 matrix at different weight fractions.

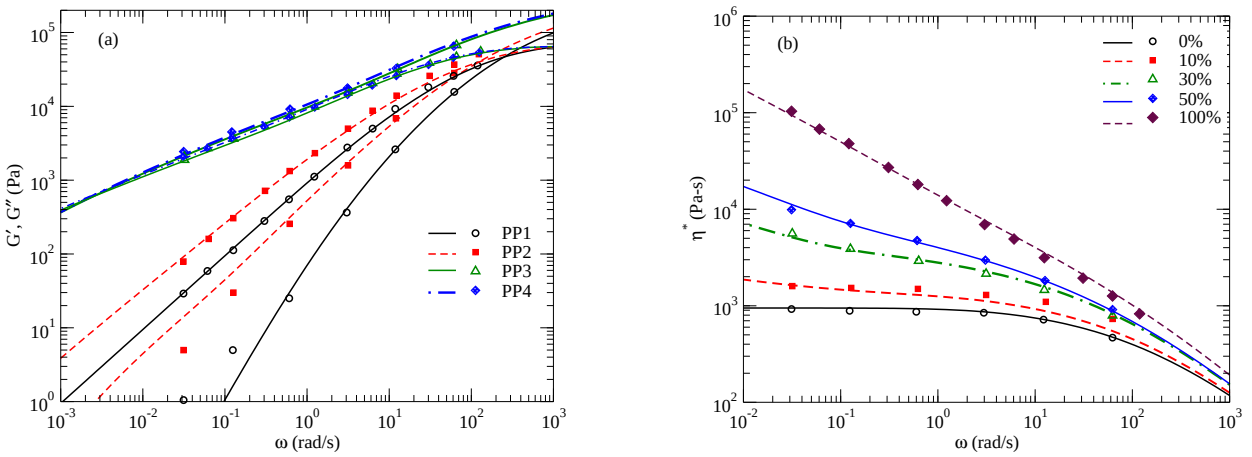

Figure 6: Frequency dependent visco-elastic moduli for the diene-propylene resins (a) and complex viscosity for various weight ratios of the branched PP4 resin in linear PP1 resin (b). Our modelling results are shown with lines. (Small angle oscillatory shear data (symbols) are reproduced with permission from Ref.[7], Ye, Z.; AlObaidi, F.; Zhu, S. *Ind. Eng. Chem. Res.*, **2004**, 43, 2860-2870. Copyright (2004) American Chemical Society.)

We define a measure of the diene content in the resins as

$$\mathrm{D_{ppm}} = 10^6 \frac{D_0 \left[1 - \exp\left(-K_{\mathrm{pD}} x_f / K_{\mathrm{p}}\right)\right]}{[\mathrm{M}] x_f}. \tag{16}$$

In the blend of PP4 and PP1, $\mathrm{D_{ppm}}$ is fixed by the weight fraction of PP4 and its diene content. Fig. 7 shows the variation of the fitted τ_e with the diene content. The plot suggests a smooth relationship between τ_e and $\mathrm{D_{ppm}}$. A similar dependence of M_e and τ_e has been observed for linear polyethylene resins with varying comonomer contents[40,41]. However, the observed change in τ_e here is orders of magnitude larger than previous observations for linear polyethylene with similar amounts of comonomer. We discuss the possible reasons for this strong dependence of τ_e on the diene content at the end of this paper.

We also explored the alternate possibility of variation in M_e. Choosing a smaller M_e for the resins with higher diene content can reproduce their low shear viscosity. But, the frequency dependence of the moduli is not predicted correctly in this case.

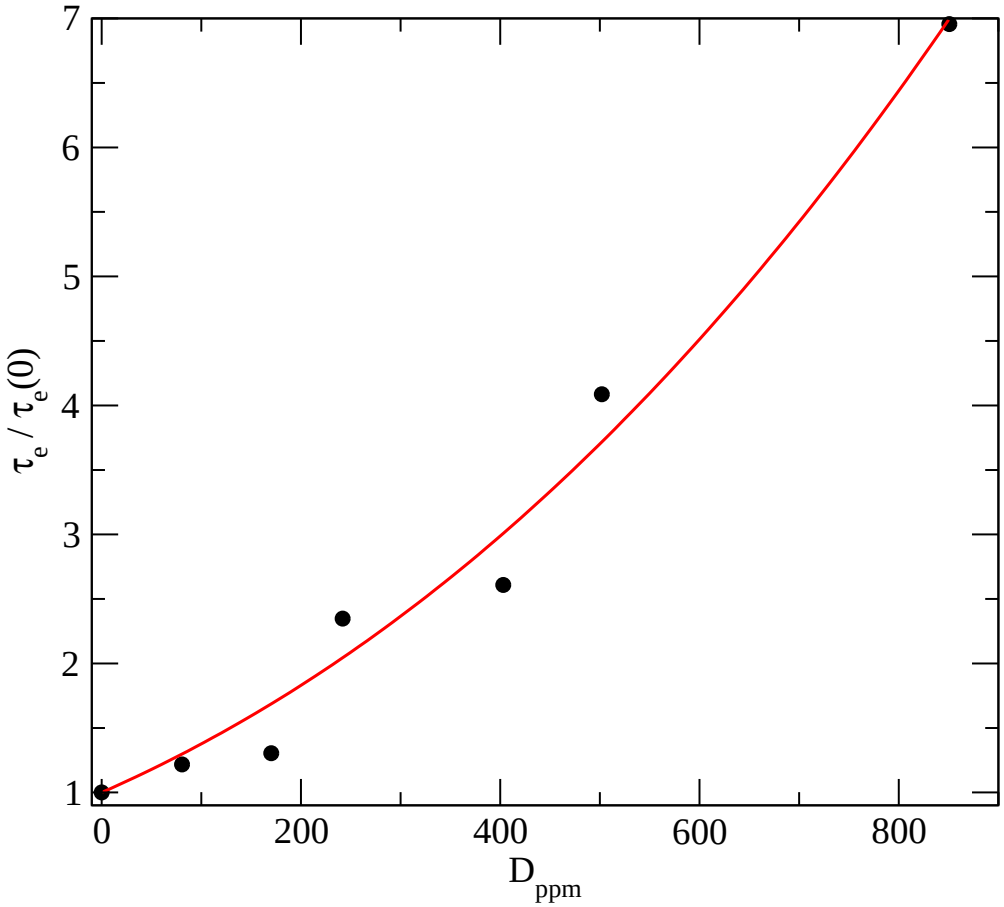

Figure 7: Dependence of τ_e on the diene content normalised by its value in absence of diene ($\tau_e(0)$). The symbols correspond to τ_e values that provide best description of the SAOS data with the diene contents (parts per million of diene monomer to propylene monomer) in the pure resins and in the blend of PP4 in PP1 (estimated from Eq. 16). The line is a fit with functional form $\tau_e/\tau_e(0) = (1 + 0.0013\mathrm{D}_{\mathrm{ppm}})^{2.6}$.

4 Discussion

Starting from simplified reaction kinetics, we have derived in this work analytical expressions for the probability distributions of the segment lengths and branching at different stages of the reaction in a semi-batch reactor for propylene-diene copolymerisation. We have used these probabilities to create ensembles of molecules using a Monte Carlo sampling. We have explored the molar mass distribution, radius of gyration contraction factor, approach to gelation, and molecular shapes as a function of initial diene concentration. Considering literature data[7] on a set of resins synthesised with varying diene concentrations, we have found good agreement with the experimentally determined molar mass distributions. Using a single additional fitting parameter, namely the entangelement time τ_e, we were able to quantitatively describe the measured visco-elastic response for the synthesised resins and their blends. The entanglement time τ_e was found to strongly depend on the diene content. The entanglement time τ_e is proportional to the molecular friction. It is possible that some fraction of the dienes undergoes local cyclization (Fig. 8a). Also, if two segments are connected by more than one diene bond, it will introduce larger cyclic segments (Fig. 8b). It is conceivable that the presence of such loops will enhance the effective molecular friction and hence τ_e. A possible question is whether a different set of reaction rate constants could fit both the molecular weight distribution and rheology data without recourse to varying τ_e. We think that this is not possible: the broadening of the molar mass distribution with increasing diene content is due to addition of branches in a particular way, and gives rise to a fairly restricted distribution of branched polymer topologies.

In our modelling, we consider dienes as small molecules that are capable of being incorporated at both ends. Thus, our model is directly applicable (with some modifications) to other branch-forming agents, like the T-reagent considered in[42]. For ethylene-diene copolymerisation with metallocene catalysts, our model needs to be extended to incorporate macromonomer induced branching[4]. In such a scenario, one would need to consider yet another rate constant for macromonomer incorporation. From the density of macromonomers,

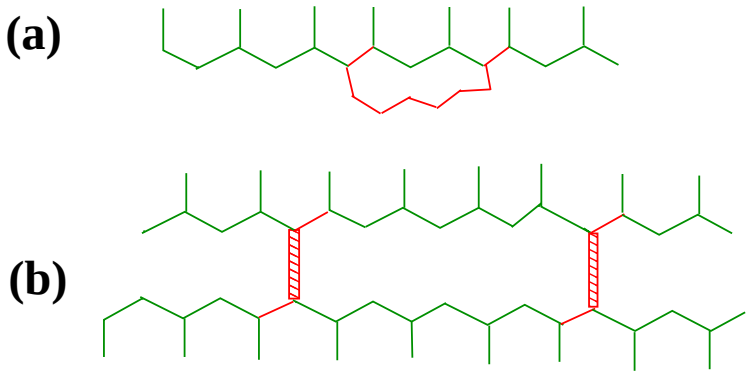

Figure 8: Possibility of loop formation in propylene-diene copolymerisation: (a) A growing chain may incorporate both ends of a diene monomer to introduce local cylization. (b) More than one diene bridges between two segments lead to longer loops.

one could calculate the average distance to a branch from macromonomer incorporation. If such a branch would be selected in the Monte Carlo step, one could calculate at which conversion the macromonomer was created and grow the macromonomer recursively. Calculations involving such simultaneous diene induced and macromonomer induced branching will be communicated in a future publication.

Appendix. Computational details

The kinetic and rheology models developed here require a number of input parameters to describe the experimental results. Simultaneous exploration of all these parameters is computationally prohibitive. In this appendix, we detail the scheme we used to constrain the parameters. We also consider alternative scenarios to those presented in the main body of the paper. While the Monte Carlo scheme for generating the molecules itself has low memory requirements, following the relaxation of branched molecules numerically is computationally costly. For all the experimental resins, we used 100000 molecules to calculate the molar mass distribution. Even for the most branched resin (PP4), the ensemble contains many linear molecules (slightly more than half of the molecules were linear). We reduce the computational load for the rheology calculation without sacrificing the accuracy by binning the linear

molecules by molar mass on a logarithmic scale using 1000 bins. Typically after this coarse-graining of the linear molecules, the ensemble of PP4 contained $\sim$ 46000 molecules. On a single Intel Xenon E5540 processor running a Linux operating system, generating 100000 molecules for PP4 takes around 45 seconds and the rheology calculations take around 50 minutes. Repeat calculations with the same parameters (but with different random seed generating independent ensemble of molecules) show that this number of molecules are sufficient to calculate the complex viscosity over the frequency range of interest within 3% variation between calculations.

The two main parameters to describe the linear rheology of entangled polymer melt for a given chemistry are the entanglement molar mass M_e and the entanglement time τ_e. We have used data on metallocene catalysed long linear iPP resin from Ref.[39] to determine these two parameters. We used BoB to generate 500000 linear polymers from a log-normal distribution with $M_w = 871000\,\mathrm{g/mol}$ and polydispersity index 2.49. M_e and τ_e were varied until the predicted viscoelastic moduli match the experimental data. The resulting fit is showed in Fig. 9.

The molar mass distribution of the linear polymers is largely determined by the ratio $\bar{K}_\mathrm{p}[\mathrm{M}]/K_\mathrm{T}$ and $\mathrm{PDI}(K_\mathrm{p})$. In particular, the low molar mass tail is determined by the ratio $\bar{K}_\mathrm{p}[\mathrm{M}]/K_\mathrm{T}$ and the width of the distribution is further modified by $\mathrm{PDI}(K_\mathrm{p})$. We estimate [M] from solubility of propylene. Since only the ratios of rate constants to $\bar{K}_\mathrm{p}$ affect the structures, we arbitrarily fix $\bar{K}_\mathrm{p} = 650\,\mathrm{L/(mol\text{-}s)}$. With this choice of $\bar{K}_\mathrm{p}$, the experimental MWD for PP1 is sufficient to set $K_\mathrm{T} = 0.085\,/\mathrm{s}$ and $\mathrm{PDI}(K_\mathrm{p}) = 1.59$. As long as K_d is not too large, its effect on the generated structure is marginal. We have used $K_\mathrm{d} = 10^{-4}\,/\mathrm{s}$ in our calculations shown here. Changing it to $K_\mathrm{d} = 10^{-3}\,/\mathrm{s}$ keeps the predictions very similar. The fact that the molecules generated with these rate constants can be used to predict the viscoelastic moduli with the M_e and τ_e determined in the previous step (Fig. 9) gives us more confidence about the structure and also about the accuracy of the GPC data (at least for the linear resin).

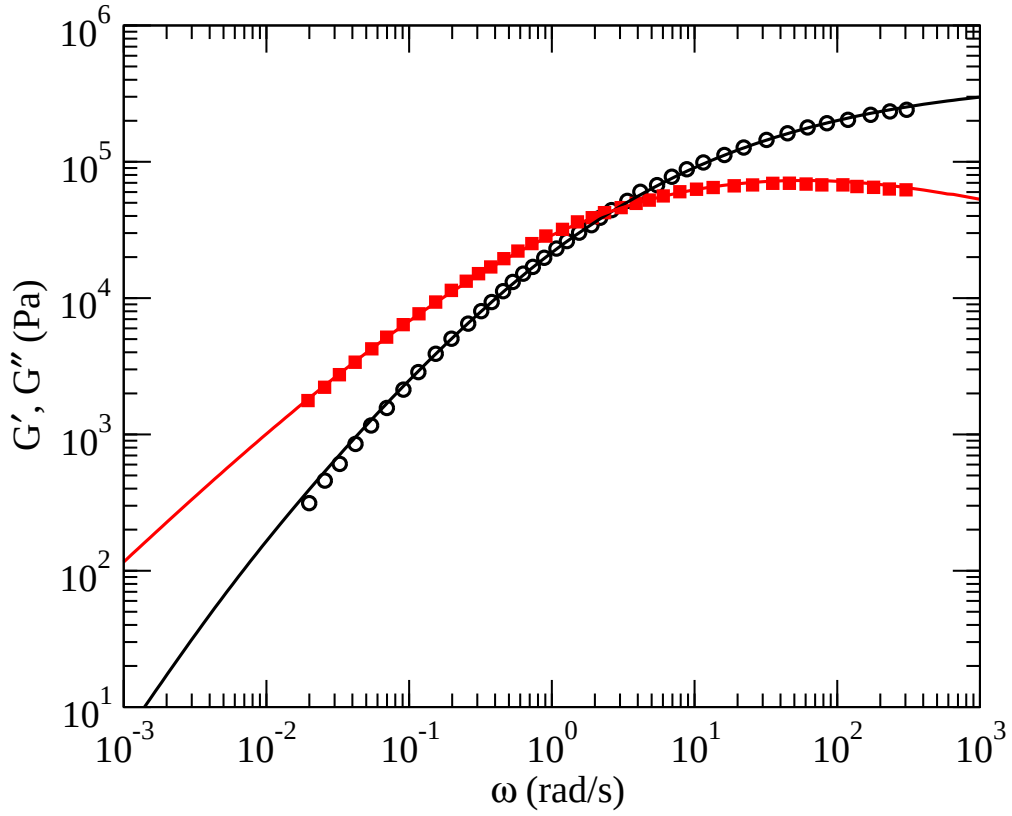

Figure 9: Fits (lines) for viscoelastic moduli of linear polymers with $M_w = 871000\,\mathrm{g/mol}$ and $PDI = 2.4$. (Experimental data (symbols) is reproduced with permission from Ref.[39], Eckstein A.; Suhm, J.; Friedrich, C.;Maier, R.-D.; Sassmannshausen, J.; Bochmann, M.; Mülhaupt, R. *Macromolecules*, **1998**, 31, 1335-1340. Copyright (1998) American Chemical Society.)

For the remaining two parameters, namely K_{pD} and K_{DLCB}, we found various combinations that describe the GPC data and the rheology data provided one resorts to changing τ_e individually for each of the resins. The change in τ_e required to describe the data varied depending on the choice of these two parameters. Among the combinations we explored, the change in τ_e was comparatively lower for $K_{\mathrm{pD}} = 180\,\mathrm{L/(mol\text{-}s)}$ and $K_{\mathrm{DLCB}} = 45\,\mathrm{L/(mol\text{-}s)}$ across the resins. For a particular branched resin, one can match the complex viscosity at some low frequency by increasing the amount of diene-induced branching. In Fig. 10 we show results from such an exercise for the most branched resin (PP4) with the theoretical predictions plotted over a much larger range of frequencies than that available for the experimental data. As a reference, we replot the viscoelastic moduli for the linear PP1. The dashed lines in the main figure show the results assuming the same τ_e for PP4 as that for PP1. The solid lines include the effect of changed τ_e to match the rheology data. The dot-dashed lines correspond to $K_{\mathrm{pD}} = 200\,\mathrm{L/(mol\text{-}s)}$ and $K_{\mathrm{DLCB}} = 30\,\mathrm{L/(mol\text{-}s)}$. The molar mass distribution (inset of Fig. 10) shows that this choice of rate constants (dashed lines) generates more branched material than the choice used in the main text (solid lines). The weight averaged molar mass increases by about 18% for this particular choice of rate constants. Though the complex viscosity from this different set of parameters matches experimental results at the lowest frequency, the overall shape remains poor and fares quite poorly at higher frequencies.

The near constant yield for all the resins (Table. 1) and the near identical shape of the GPC data at the low molar mass end (Fig. 5) suggest that the linear segments are identical for all the resins. Without increasing the length of the segments, increasing the amount of branching does not slow down the predicted relaxation above $\sim 20000\,\mathrm{rad/s}$ (relaxation at these frequencies is dominated by arm retraction of the outer segments). Thus, it is very unlikely for the predicted modulus to remain as high as in the experimental data for the branched resins, with τ_e being held constant. For this reason, we are confident in our conclusion that τ_e changes with increased diene content.

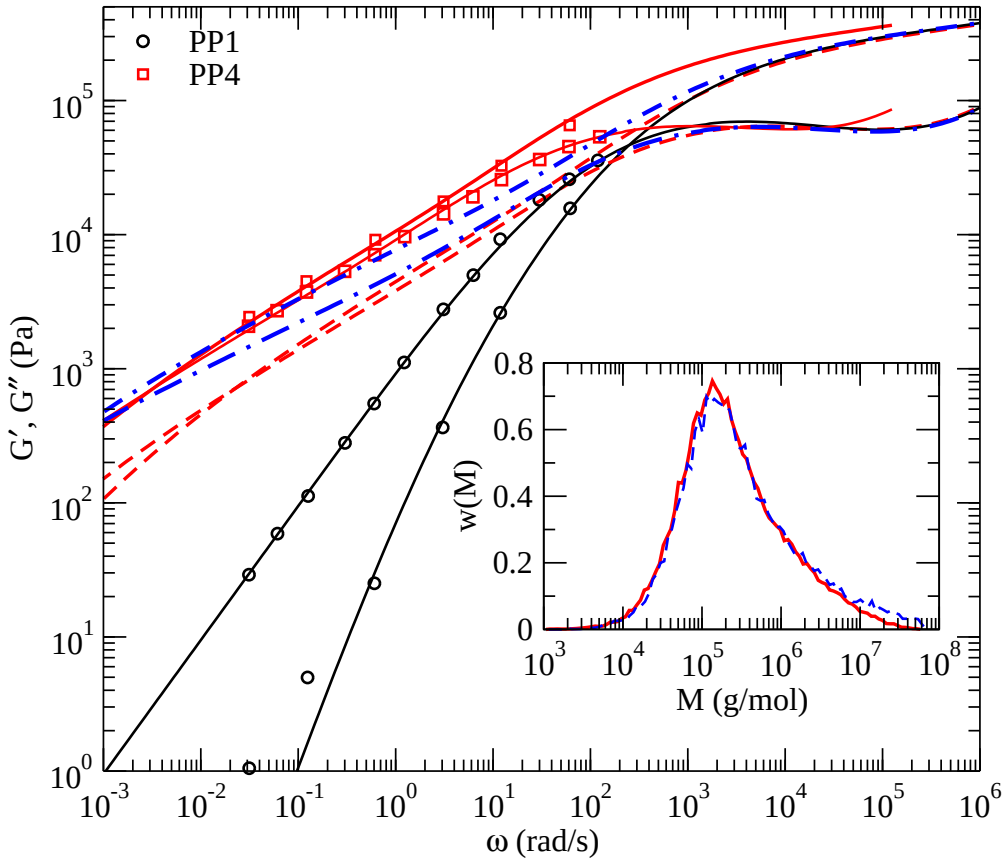

Figure 10: Effect of increased branching on rheology (main plot) and molar mass distribution (inset). Experimental rheology results (symbols) and predictions (lines) for linear resin PP1 are shown as reference. For PP4, we show a number of predictions with different choice of parameters (see text).

Acknowledgements

We thank João Soares and Tom McLeish for useful discussions.

References

(1) Yan, D.; Wang, W. J.; Zhu, S. *Polymer* **1999**, *40*, 1737–1744.

(2) Gotsis, A. D.; Zeevenhoven, B. L. F.; Hogt, A. H. *Polymer Eng. Sc.* **2004**, *44*, 973–982.

(3) Braunschweig, H.; Breitling, F. M. *Coordination Chemistry Reviews* **2006**, *250*, 2691–2720.

(4) Soares, J. B. P.; Hamielec, A. E. *Macromol. Theory Simul.* **1996**, *5*, 547–572.

(5) Resconi, L.; Piemontesi, F.; Franciscono, G.; Abis, L.; Fiorani, T. *J. Am. Chem. Soc.* **1992**, *114*, 1025–1032.

(6) Kawahara, N.; Kojoh, S.-i.; Matsuo, S.; Kaneko, H.; Matsugi, T.; Toda, Y.; Mizuno, A.; Kashiwa, N. *Polymer* **2004**, *45*, 2883–2888.

(7) Ye, Z.; AlObaidi, F.; Zhu, S. *Ind. Eng. Chem. Res.* **2004**, *43*, 2860–2870.

(8) Paavola, S.; Saarinen, T.; Löfgren, B.; Pitkänen, P. *Polymer* **2004**, *45*, 2099–2110.

(9) Agarwal, P. K.; Weng, W.; Mehta, A. K.; Dekmezian, A. H.; Chang, M.; Chudgar, R. K.; Davey, C. R.; Lin, C. Y.; Chen, M. C.; Richeson, G. C.; Weng, W. Articles formed from propylene diene copolymers. 2004; EP Patent 1,237,963.

(10) Pietikäinen, P.; Seppälä, J. V.; Ahjopalo, L.; Pietilä, L.-O. *Eur. Poly. J.* **2000**, *36*, 183–192.

(11) Guzmán, J. D.; Arriola, J., Daniel; Karjala, T.; Gaubert, J.; Kolthammer, B. W. S. *AIChE J.* **2010**, *56*, 1325–1333.

(12) Cozewith, C.; Graessley, W. W.; ver Strate, G. *Chem. Eng. Sc.* **1979**, *34*, 245–248.

(13) ver Strate, G.; Cozewith, C.; Graessley, W. W. *J. Appl. Polymer Sc.* **1980**, *25*, 59–62.

(14) Li, R.; Corripio, A. B.; Dooley, K. M.; Henson, M. A.; Kurtz, M. J. *Chem. Eng. Sc.* **2004**, *59*, 2297–2313.

(15) Nele, M.; Soares, J. B. P.; Pinto, J. C. *Macromol. Theory Simul.* **2003**, *12*, 582–592.

(16) Dias, R. C. S.; Costa, M. R. P. F. N. *Macromol. React. Eng.* **2007**, *1*, 440–467.

(17) Larson, R. G. *Macromolecules* **2001**, *34*, 4556–4571.

(18) Park, S. J.; Shanbhag, S.; Larson, R. G. *Rheol. Acta* **2005**, *44*, 319–330.

(19) Das, C.; Inkson, N. J.; Read, D. J.; Kelmanson, M. A.; McLeish, T. C. B. *J. Rheol.* **2006**, *50*, 207–235.

(20) van Ruymbeke, E.; Bailly, C.; Keunings, R.; Vlassopoulos, D. *Macromolecules* **2006**, *39*, 6248–6259.

(21) Read, D. J.; Auhl, D.; Das, C.; den Doelder, J.; Kapnistos, M.; Vittorias, I.; McLeish, T. C. B. *Science* **2011**, *333*, 1871–1874.

(22) Das, C.; Read, D. J.; Auhl, D.; Kapnistos, M.; den Doelder, J.; Vittorias, I.; McLeish, T. C. B. *J. Rheol.* **2014**, *58*, 737–757.

(23) Doi, M.; Edwards, S. F. *The theory of polymer dynamics*; Clarendon Press: Oxford, 1986.

(24) Read, D. J.; McLeish, T. C. B. *Macromolecules* **2001**, *34*, 1928–1945.

(25) Inkson, N. J.; Das, C.; Read, D. J. *Macromolecules* **2006**, *39*, 4920–4931.

(26) Tobita, H. *J. Polymer Sc. B.* **2001**, *39*, 391–403.

(27) Tobita, H. *Macromol. React. Eng.* **2013**, *7*, 181–192.

(28) McLeish, T. C. B.; Larson, R. G. *J. Rheol.* **1998**, *42*, 81–110.

(29) Atiqullah, M.; Hammawa, H.; Hamid, H. *Eur. Polym. J.* **1998**, *34*, 1511–1520.

(30) Bergstra, M.; Weickert, G.; Meier, G. B. *Macromolecular reaction Engineering* **2009**, *3*, 433–447.

(31) bob2.5. `http://sourceforge.net/bob-rheology`, 2012.

(32) Das, C.; Read, D. J.; Kelmanson, M. A.; McLeish, T. *Phys. Rev. E* **2006**, *74*, 011404.

(33) den Doelder, J.; Das, C.; Read, D. J. *Rheo. Acta.* **2011**, *50*, 469–484.

(34) Milner, S. T.; McLeish, T. C. B. *Macromolecules* **1997**, *30*, 2159–2166.

(35) Marrucci, G. *J. Polym. Sci., Polym. Phys. Ed.* **1985**, *23*, 159–177.

(36) Viovy, J. L.; Rubinstein, M.; Colby, R. H. *Macromolecules* **1991**, *24*, 3587–3596.

(37) Milner, S. T.; McLeish, T. C. B.; Young, R. N.; Hakiki, A.; Johnson, J. M. *Macromolecules* **1998**, *31*, 9345–9353.

(38) Wang, Z.; Chen, X.; Larson, R. G. *J. Rheol.* **2010**, *54*, 223–260.

(39) Eckstein, A.; Suhm, J.; Friedrich, C.; Maier, R. D.; Sassmannshausen, J.; Bochmann, M.; Mülhaupt, R. *Macromolecules* **1998**, *31*, 1335–1340.

(40) Fetters, L. J.; Lohse, D. J.; García-Franco, C. A.; Brant, P.; Richter, D. *Macromolecules* **2002**, *35*, 10096–10101.

(41) Chen, X.; Stadler, F. J.; Münstedt, H.; Larson, R. G. *J. Rheol.* **2010**, *54*, 393–406.

(42) Langston, J. A.; Colby, R. H.; Chung, T. C. M.; Shimizu, F.; Suzuki, T.; Aoki, M. *Macromolecules* **2007**, *40*, 2712–2720.

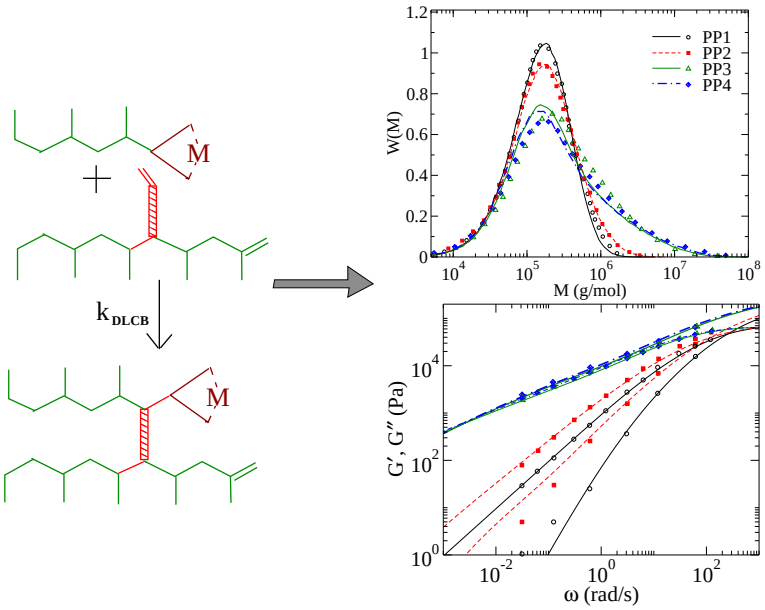

For Table of Contents use only

Title: "Modelling of synthesis and flow properties of propylene-diene copolymers"

Authors: Chinmay Das, Daniel J. Read, Johannes M. Soulages and Pradeep P. Shirodkar